Supplementary Fig. S1

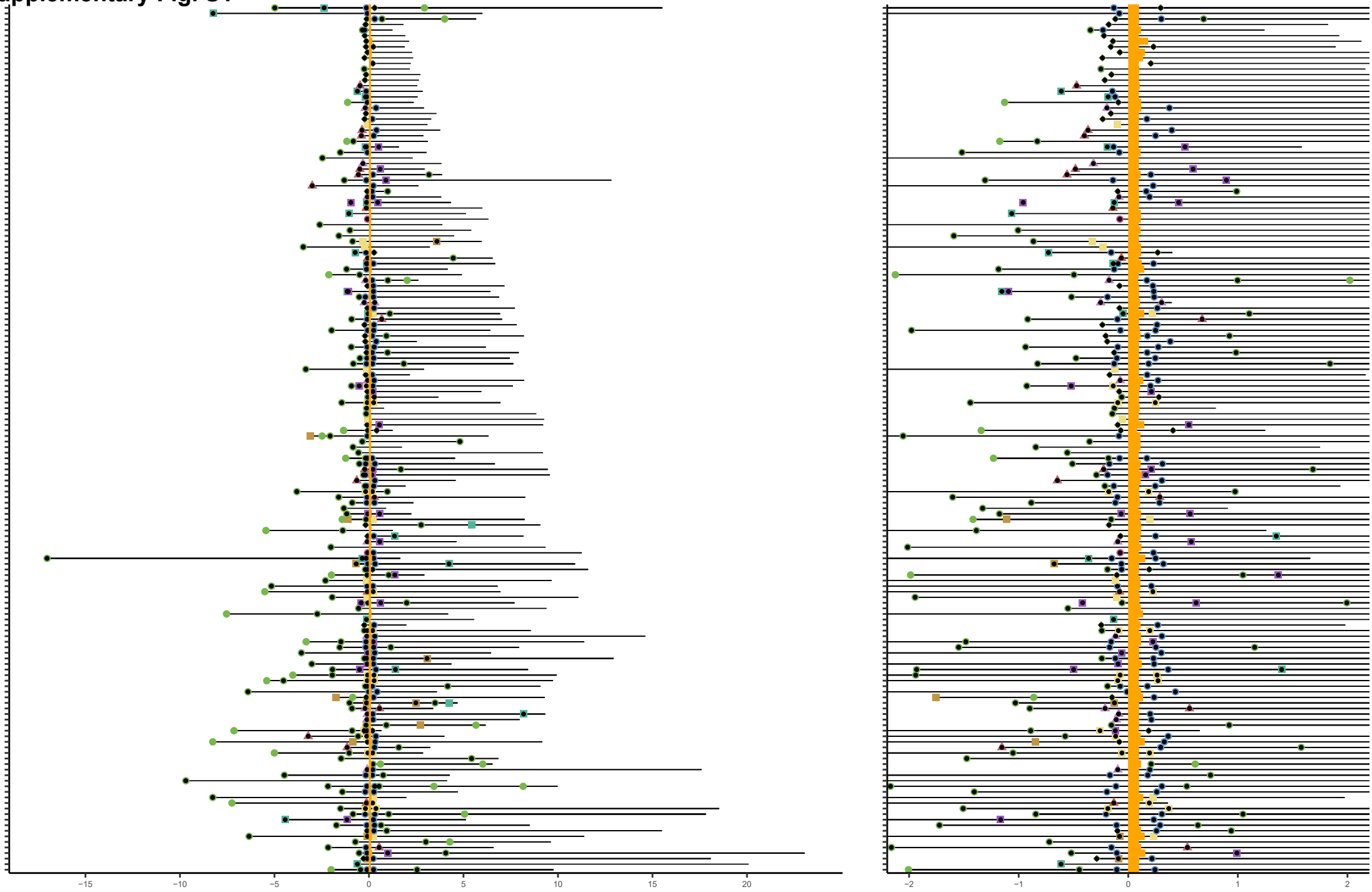

Supplementary Fig. S1

Detailed overview of patients disease courses and analyzed samples. Lines represent patient's disease courses from time of first analyzed tumor or urine sample to end of FU centered around the first induction treatment of BCG with at least five instillations. Colors indicate performed analyses. Shapes indicate the number of analyses per clinical timepoint. Left: full FU. Right: Two years pre and post-BCG illustrated.

Supplementary Fig. S2

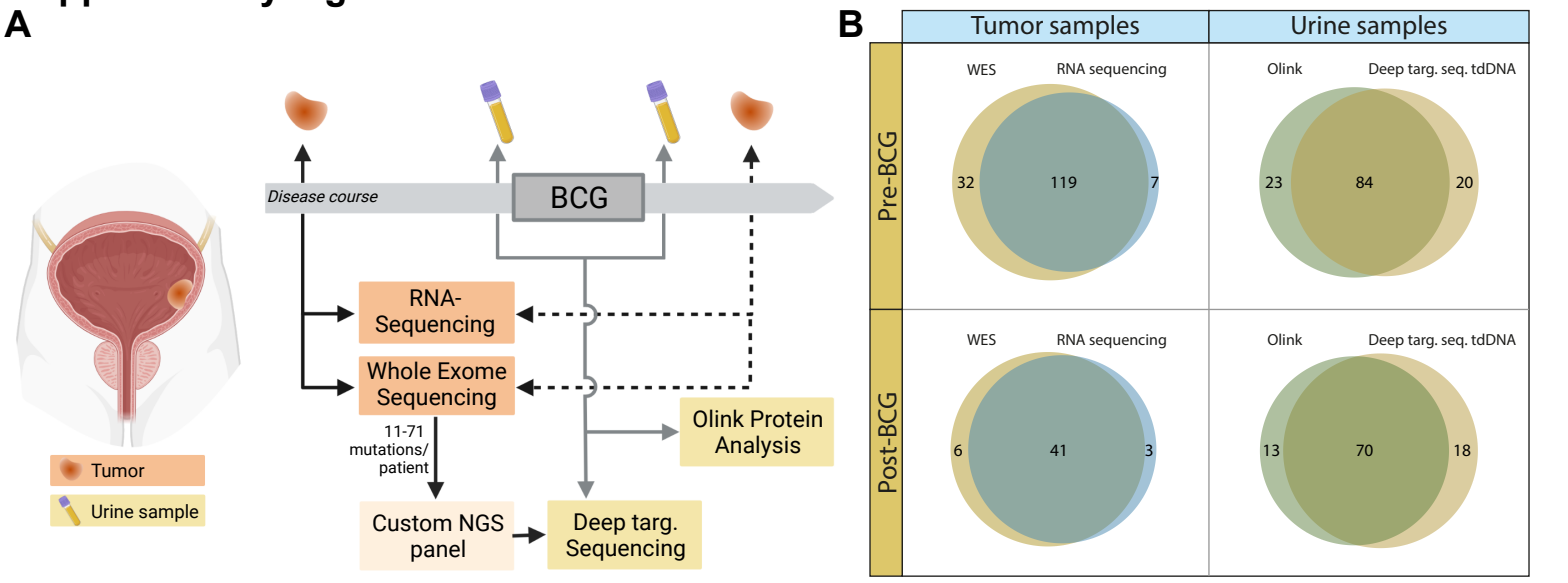

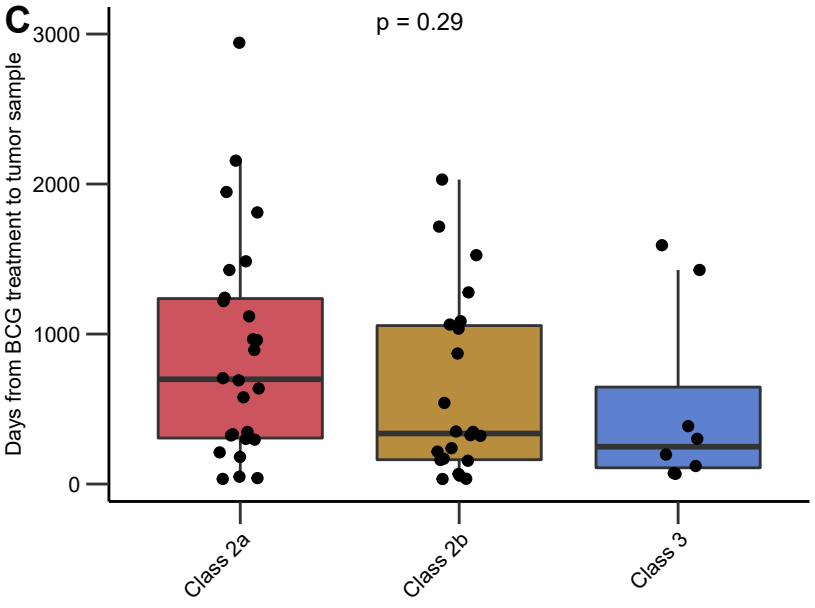

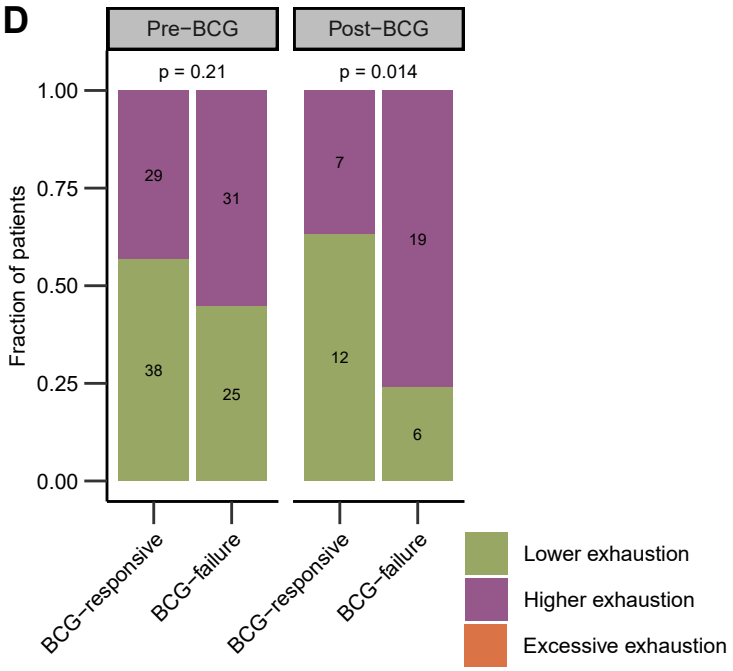

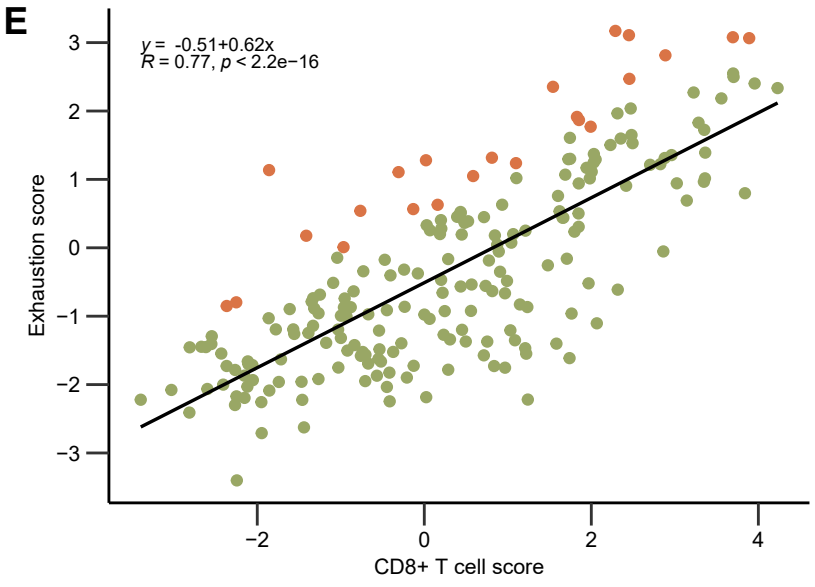

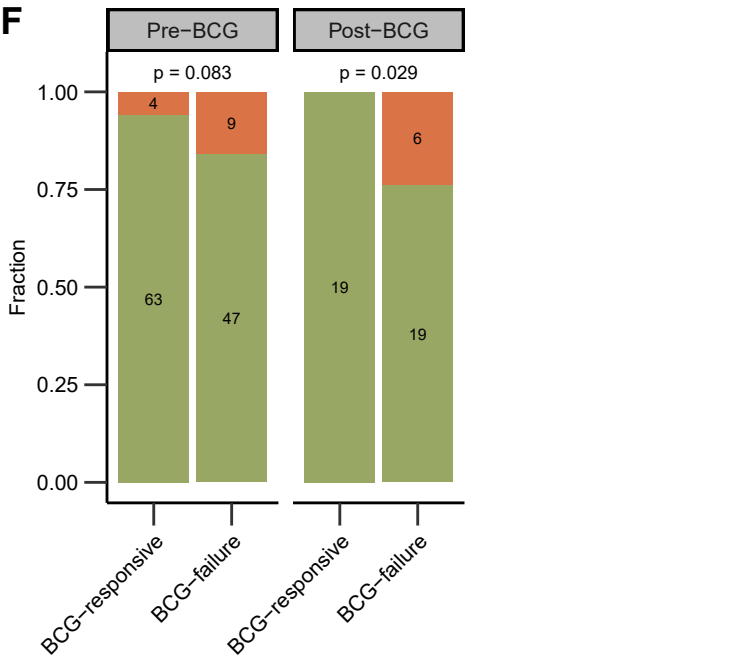

Supplementary Fig. S2

Study and sample overview and RNAseq based analyses. A) Overview of study with disease course including BCG treatment of at least five instillations and sample types at different time points. Dashed lines indicate samples analyzed from a limited number of patients. Design of custom panel for deep targeted sequencing is outlined. Created with BioRender.com (publication license obtained). B) Venn diagram showing overlapping samples between analysis methods. C) Association between UROMOL2021 tumor subtype and time from BCG treatment for all post-BCG samples sequenced for the project (Wilcoxon Rank Sum test). D) CD8 adjusted exhaustion status in BCG-responsive and BCG-failure patients in pre- and post-BCG tumors, respectively (Fisher's Exact test). E) Correlation between CD8 T-cell score and exhaustion score. Green = lower exhaustion (residuals <=1.04). Purple = excessive exhaustion (residuals >1.04). Pearson correlation was used to determine the correlation coefficient *R* and *p*-value. F) Excessive exhaustion status in BCG-responsive and BCG-failure patients in pre- and post-BCG tumors, respectively (Fisher's Exact test).

Supplementary Fig. S3

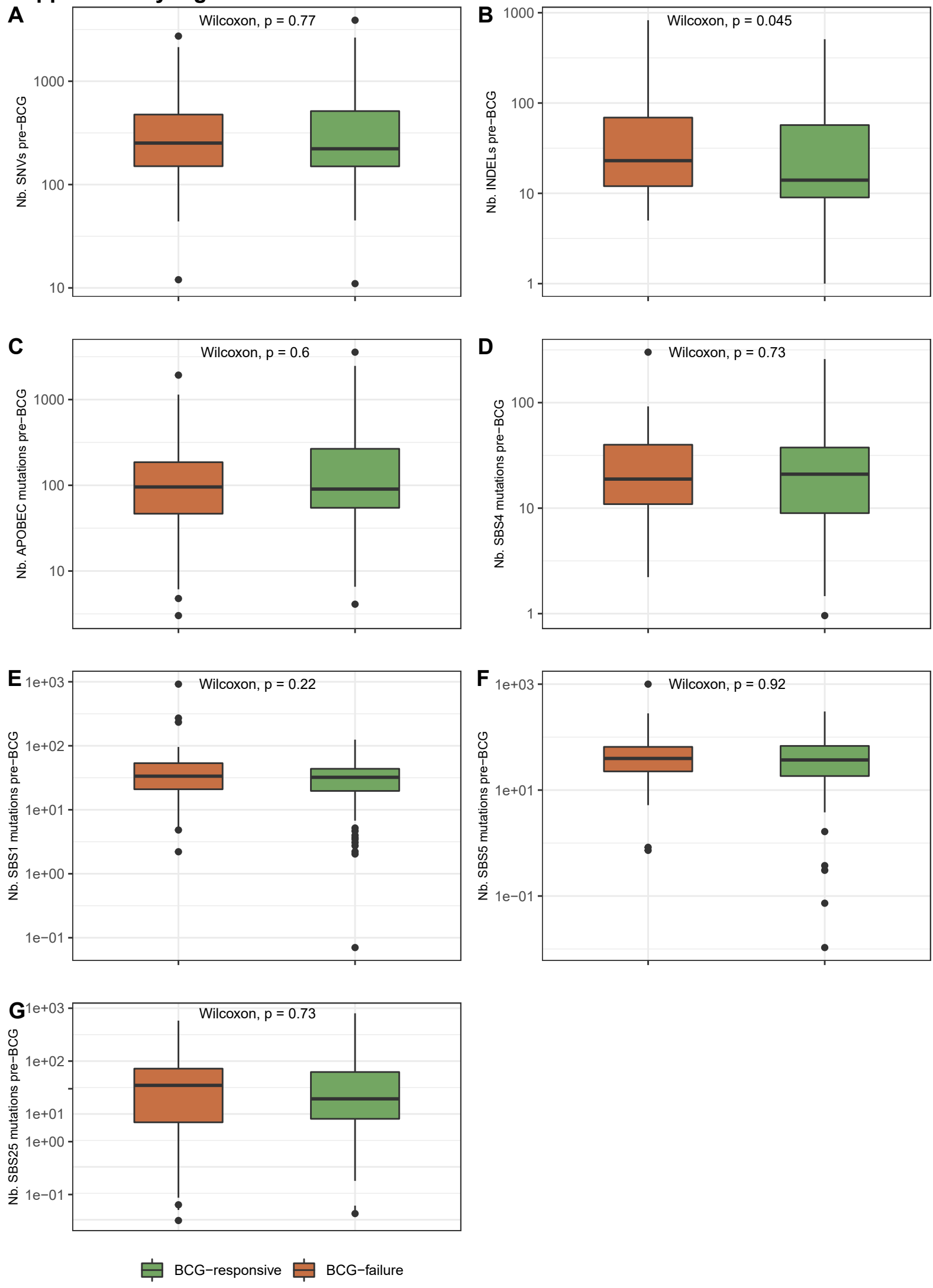

Supplementary Fig. S3

Correlations between tumor WES characteristics and BCG-response. A) The number of single nucleotide variants (SNVs) in pre-BCG tumor samples correlated to response to BCG. B) The number of INDELs in pre-BCG tumor samples correlated to response to BCG. C) The number of APOBEC-related mutations (SBS2+SBS13) in pre-BCG tumor samples correlated to response to BCG. D) The number of SBS4-related mutations in pre-BCG tumor samples correlated to response to BCG. E) The number of SBS1-related mutations in pre-BCG tumor samples correlated to response to BCG. F) The number of SBS5-related mutations in pre-BCG tumor samples correlated to response to BCG. G) The number of SBS25-related mutations in pre-BCG tumor samples correlated to response to BCG. Green = BCG-responsive patients. Orange = BCG-failure patients. The Wilcoxon Rank Sum test was used for statistical comparisons.

Supplementary Fig. S4

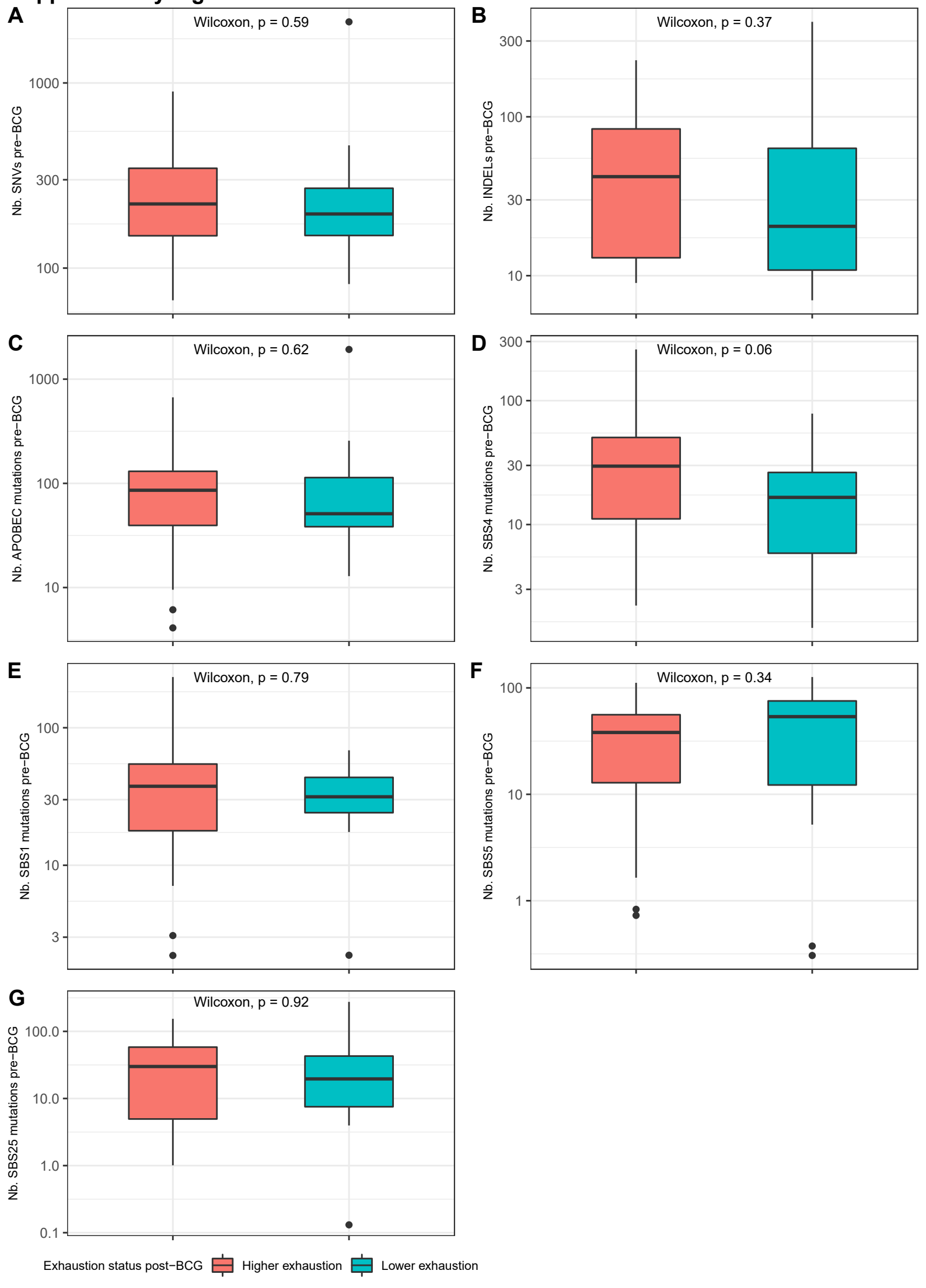

Supplementary Fig. S4

Correlations between post-BCG tumor exhaustion status and pre-BCG tumor WES characteristics. A) The number of single nucleotide variants (SNVs) in pre-BCG tumor samples correlated to post-BCG exhaustion status. B) The number of INDELs in pre-BCG tumor samples correlated to post-BCG exhaustion status. C) The number of APOBEC-related mutations (SBS2+SBS13) in pre-BCG tumor samples correlated to post-BCG exhaustion status. D) The number of SBS4-related mutations in pre-BCG tumor samples correlated to post-BCG exhaustion status. E) The number of SBS1-related mutations in pre-BCG tumor samples correlated to post-BCG exhaustion status. F) The number of SBS5-related mutations in pre-BCG tumor samples correlated to post-BCG exhaustion status. G) The number of SBS25-related mutations in pre-BCG tumor samples correlated to post-BCG exhaustion status. Pink = Higher post-BCG exhaustion. Turquoise = Lower post-BCG exhaustion. The Wilcoxon Rank Sum test was used for statistical comparisons.

Supplementary Fig. S5

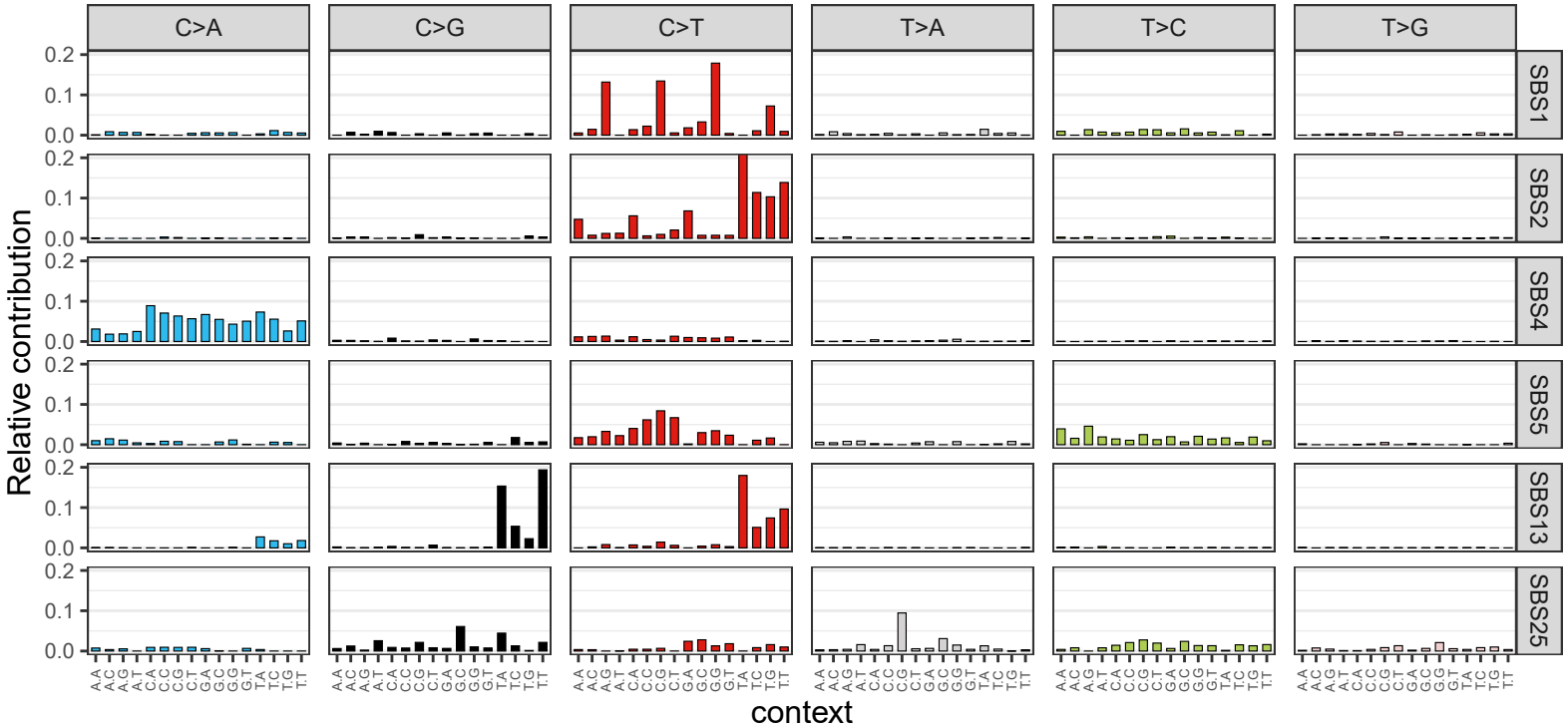

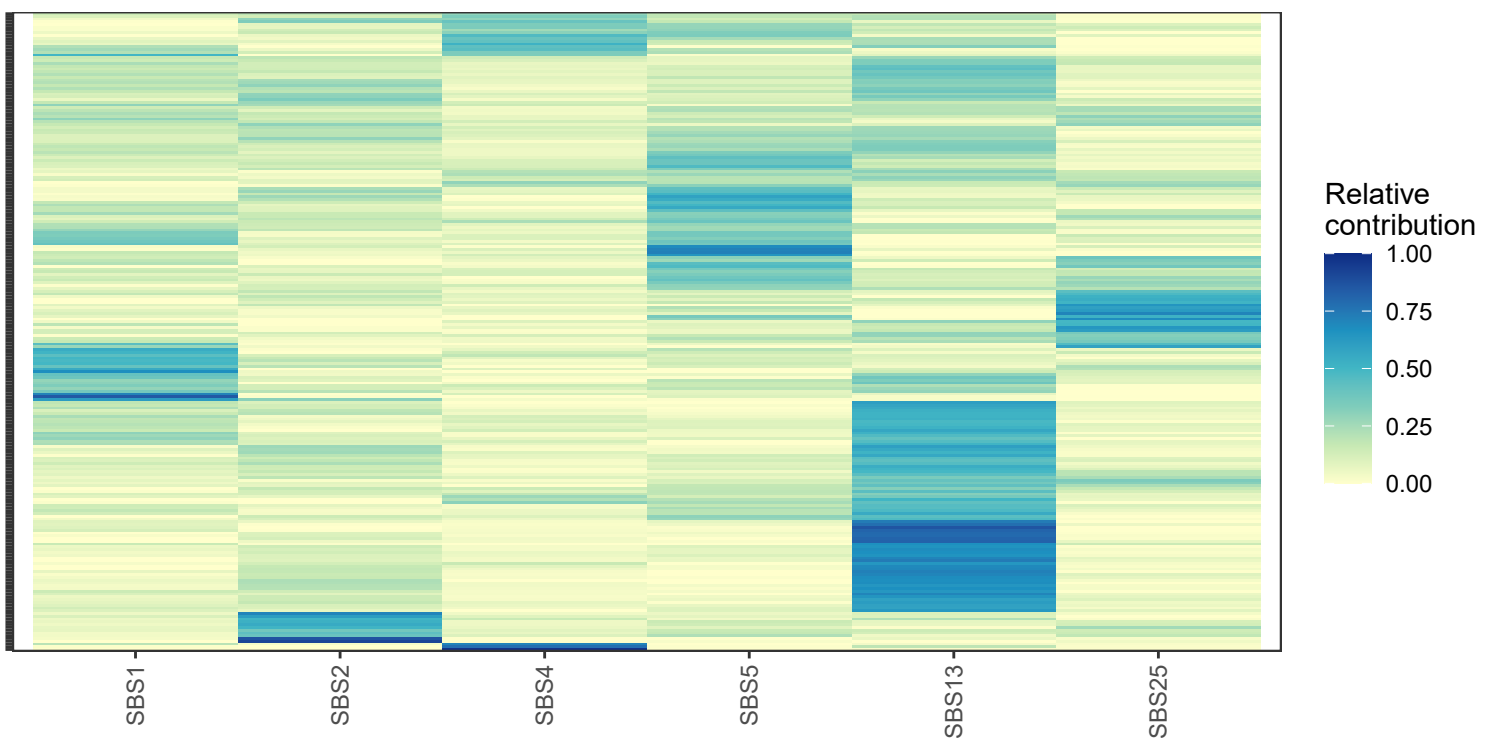

Supplementary Fig. S5

Overview of identified mutational signatures. A) Detailed mutational profiles for the six mutational signatures identified by de novo extraction using the R package MutationalPatterns. Extracted signatures were named according to COSMIC signatures with the highest resemblance, as estimated using cosine similarity and resulting in the following values: SBS1 = 0.91, SBS2, 0.92, SBS4 = 0.89, SBS5 = 0.75, SBS13 = 0.76, SBS25 = 0.64. B) Relative contribution of the identified mutational signatures. Sample clustering was performed based on euclidean distances.

Supplementary Table S1: Olink proteins and results

Overview of analyzed proteins using the Olink proteomics platform and associated biological processes. P-values and Benjamini-Hochberg adjusted P-values from paired t-tests for comparisons between pre-BCG and post-BCG samples for all patients, BCG-responsive patients, and patients with BCG-failure are shown. Green color indicates p-values < 0.05 and blue color indicates q-values <0.1.

Olink Information				All Patients		BCG-responsive		BCG-failure		Test
Assay	*OlinkID*	*UniProt*	*Biological process*	*P-value*	*Adjusted p-value*	*P-value*	*Adjusted p-value*	*P-value*	*Adjusted p-value*	*Method*
ADA	OID00775	P00813	Metabolism	2,47E-02	9,91E-02	4,12E-02	3,70E-01	1,83E-01	3,11E-01	Paired t-test
ADGRG1	OID00764	Q9Y653	Vascular and tissue remodeling	4,50E-02	1,22E-01	8,40E-01	9,94E-01	2,38E-02	1,37E-01	Paired t-test
ANGPT1	OID00760	Q15389	Vascular and tissue remodeling	9,39E-01	9,71E-01	6,89E-01	9,76E-01	7,24E-01	7,66E-01	Paired t-test
ANGPT2	OID00822	O15123	Vascular and tissue remodeling	9,99E-01	9,99E-01	1,17E-01	5,68E-01	4,72E-01	5,37E-01	Paired t-test
ARG1	OID00815	P05089	Suppresses tumor immunity	8,70E-02	1,96E-01	7,42E-01	9,76E-01	8,75E-02	2,24E-01	Paired t-test
CAIX	OID00773	Q16790	Metabolism; Vascular and tissue remodeling	2,37E-01	3,63E-01	9,32E-01	9,94E-01	1,02E-01	2,34E-01	Paired t-test
CASP-8	OID00827	Q14790	Apoptosis/cell killing	5,17E-01	5,81E-01	7,78E-01	9,76E-01	3,83E-01	4,90E-01	Paired t-test
CCL17	OID00821	Q92583	Chemotaxis; Suppresses tumor immunity	4,45E-01	5,25E-01	5,12E-01	9,01E-01	1,66E-01	3,02E-01	Paired t-test
CCL19	OID00794	Q99731	Chemotaxis; Suppresses tumor immunity	6,66E-04	1,14E-02	4,27E-02	3,70E-01	7,09E-03	7,44E-02	Paired t-test
CCL20	OID00837	P78556	Chemotaxis; Suppresses tumor immunity	3,75E-02	1,11E-01	3,40E-02	3,70E-01	1,55E-01	2,90E-01	Paired t-test
CCL23	OID00811	P55773	Chemotaxis; Vascular and tissue remodeling	1,11E-04	2,55E-03	6,67E-03	1,16E-01	5,56E-03	7,31E-02	Paired t-test
CCL3	OID00813	P10147	Chemotaxis	2,22E-01	3,53E-01	3,37E-01	7,53E-01	3,48E-01	4,78E-01	Paired t-test
CCL4	OID00796	P13236	Chemotaxis	2,66E-02	9,91E-02	5,55E-02	4,26E-01	1,16E-01	2,38E-01	Paired t-test
CD244	OID00758	Q9BZW8	Promotes tumor immunity; Promotes tumor immunity	2,84E-01	4,08E-01	8,71E-01	9,94E-01	9,24E-02	2,24E-01	Paired t-test
CD27	OID00800	P26842	Promotes tumor immunity	2,89E-02	9,91E-02	3,12E-01	7,53E-01	5,02E-02	1,75E-01	Paired t-test
CD28	OID00793	P10747	Promotes tumor immunity	3,30E-01	4,40E-01	7,27E-01	9,76E-01	3,41E-01	4,75E-01	Paired t-test
CD4	OID00776	P01730	Promotes tumor immunity; Suppresses tumor immunity	6,77E-02	1,67E-01	5,19E-01	9,01E-01	5,85E-02	1,75E-01	Paired t-test
CD40	OID00781	P25942	Promotes tumor immunity	9,46E-03	6,69E-02	2,55E-01	6,90E-01	1,64E-02	1,00E-01	Paired t-test
CD40-L	OID00756	P29965	Apoptosis/cell killing; Promotes tumor immunity	8,03E-01	8,49E-01	6,52E-01	9,76E-01	9,35E-01	9,45E-01	Paired t-test
CD5	OID00812	P06127	Promotes tumor immunity; Suppresses tumor immunity	1,96E-03	1,81E-02	1,50E-01	5,87E-01	4,57E-03	7,31E-02	Paired t-test
CD70	OID00808	P32970	Promotes tumor immunity	7,48E-04	1,14E-02	3,24E-01	7,53E-01	6,56E-04	1,51E-02	Paired t-test
CD83	OID00841	Q01151	Promotes tumor immunity	2,96E-03	2,47E-02	2,13E-01	6,56E-01	5,46E-03	7,31E-02	Paired t-test
CD8A	OID00772	P01732	Promotes tumor immunity	1,60E-02	8,20E-02	1,53E-01	5,87E-01	5,55E-02	1,75E-01	Paired t-test
CRTAM	OID00766	O95727	Promotes tumor immunity	1,05E-01	2,25E-01	6,00E-01	9,76E-01	1,12E-02	8,33E-02	Paired t-test
CSF-1	OID00843	P09603	Suppresses tumor immunity	1,66E-01	3,03E-01	8,25E-01	9,94E-01	1,06E-01	2,38E-01	Paired t-test
CX3CL1	OID00806	P78423	Chemotaxis; Promotes tumor immunity	2,07E-02	9,52E-02	8,47E-01	9,94E-01	8,02E-03	7,44E-02	Paired t-test
CXCL1	OID00786	P09341	Chemotaxis; Suppresses tumor immunity; Vascular and tissue remodeling	4,40E-02	1,22E-01	4,53E-01	8,34E-01	6,28E-02	1,75E-01	Paired t-test
CXCL10	OID00807	P02778	Chemotaxis; Promotes tumor immunity; Vascular and tissue remodeling	3,12E-09	9,58E-08	6,87E-05	2,11E-03	1,23E-05	3,78E-04	Paired t-test
CXCL11	OID00767	O14625	Chemotaxis; Promotes tumor immunity; Suppresses tumor immunity; Vascular and tissue remodeling	6,50E-11	3,01E-09	7,25E-06	3,33E-04	1,58E-06	1,45E-04	Paired t-test
CXCL12	OID00824	P48061	Chemotaxis; Suppresses tumor immunity; Vascular and tissue remodeling	7,49E-01	8,01E-01	4,26E-01	8,16E-01	7,77E-01	8,12E-01	Paired t-test
CXCL13	OID00830	O43927	Chemotaxis; Promotes tumor immunity; Suppresses tumor immunity	1,10E-02	7,24E-02	2,14E-01	6,56E-01	2,63E-02	1,42E-01	Paired t-test
CXCL5	OID00801	P42830	Chemotaxis; Suppresses tumor immunity; Vascular and tissue remodeling	3,74E-01	4,71E-01	7,18E-01	9,76E-01	4,21E-01	5,16E-01	Paired t-test
CXCL9	OID00771	Q07325	Chemotaxis; Promotes tumor immunity; Vascular and tissue remodeling	4,70E-11	3,01E-09	2,21E-06	2,03E-04	5,41E-06	2,49E-04	Paired t-test
DCN	OID00817	P07585	Vascular and tissue remodeling	1,08E-01	2,27E-01	8,83E-01	9,94E-01	5,26E-02	1,75E-01	Paired t-test
EGF	OID00759	P01133	Vascular and tissue remodeling	1,73E-01	3,07E-01	7,75E-01	9,76E-01	4,94E-02	1,75E-01	Paired t-test
FASLG	OID00792	P48023	Apoptosis/cell killing	1,26E-02	7,25E-02	1,07E-01	5,45E-01	5,29E-02	1,75E-01	Paired t-test
FGF2	OID00770	P09038	Vascular and tissue remodeling	3,04E-02	9,91E-02	1,78E-01	6,18E-01	9,56E-02	2,25E-01	Paired t-test
Gal-1	OID00798	P09382	Suppresses tumor immunity	6,91E-01	7,48E-01	7,27E-01	9,76E-01	4,72E-01	5,37E-01	Paired t-test
Gal-9	OID00779	O00182	Apoptosis/cell killing; Suppresses tumor immunity; Vascular and tissue remodeling	3,81E-01	4,72E-01	8,44E-02	4,85E-01	9,01E-01	9,21E-01	Paired t-test
GZMA	OID00804	P12544	Apoptosis/cell killing	1,22E-02	7,25E-02	7,58E-03	1,16E-01	6,19E-02	1,75E-01	Paired t-test
GZMB	OID00840	P10144	Apoptosis/cell killing	2,74E-02	9,91E-02	8,41E-02	4,85E-01	1,21E-01	2,43E-01	Paired t-test
GZMH	OID00783	P20718	Apoptosis/cell killing	1,68E-01	3,03E-01	6,47E-01	9,76E-01	1,96E-01	3,28E-01	Paired t-test
HGF	OID00803	P14210	Vascular and tissue remodeling	2,99E-02	9,91E-02	3,51E-01	7,53E-01	4,35E-02	1,75E-01	Paired t-test
HO-1	OID00805	P09601	Metabolism	9,41E-01	9,71E-01	9,46E-01	9,94E-01	9,67E-01	9,67E-01	Paired t-test
ICOSLG	OID00828	O75144	Promotes tumor immunity	3,14E-02	9,91E-02	7,51E-01	9,76E-01	1,18E-02	8,33E-02	Paired t-test
IFN-gamma	OID05552	P01579	Promotes tumor immunity	4,40E-01	5,25E-01	3,76E-01	7,53E-01	8,13E-01	8,40E-01	Paired t-test
IL-1 alpha	OID00757	P01583	Promotes tumor immunity; Suppresses tumor immunity; Vascular and tissue remodeling	2,92E-01	4,13E-01	4,08E-01	7,98E-01	4,53E-01	5,34E-01	Paired t-test
IL10	OID00809	P22301	Suppresses tumor immunity	9,52E-01	9,71E-01	3,75E-01	7,53E-01	6,84E-01	7,49E-01	Paired t-test
IL12	OID00842	P29459,P29460	Promotes tumor immunity	8,20E-02	1,93E-01	3,64E-01	7,53E-01	1,43E-01	2,79E-01	Paired t-test
IL12RB1	OID00835	P42701	Promotes tumor immunity	4,48E-02	1,22E-01	2,28E-01	6,56E-01	1,13E-01	2,38E-01	Paired t-test
IL13	OID00836	P35225	Suppresses tumor immunity	4,61E-01	5,36E-01	9,93E-01	9,94E-01	3,64E-01	4,78E-01	Paired t-test
IL15	OID05551	P40933	Chemotaxis; Promotes tumor immunity; Suppresses tumor immunity	6,83E-01	7,48E-01	9,94E-01	9,94E-01	5,81E-01	6,43E-01	Paired t-test
IL18	OID00782	Q14116	Promotes tumor immunity; Suppresses tumor immunity	1,56E-01	3,03E-01	2,36E-01	6,58E-01	4,06E-01	5,12E-01	Paired t-test
IL2	OID00778	P60568	Promotes tumor immunity	3,66E-01	4,71E-01	9,78E-01	9,94E-01	2,71E-01	4,04E-01	Paired t-test
IL33	OID00788	O95760	Suppresses tumor immunity	2,43E-01	3,66E-01	9,27E-01	9,94E-01	1,51E-01	2,89E-01	Paired t-test
IL4	OID00833	P05112	Suppresses tumor immunity	2,75E-01	4,02E-01	6,31E-01	9,76E-01	2,99E-01	4,37E-01	Paired t-test
IL5	OID00802	P05113	Suppresses tumor immunity	1,24E-01	2,47E-01	1,81E-01	6,18E-01	3,56E-01	4,78E-01	Paired t-test
IL6	OID00763	P05231	Promotes tumor immunity; Suppresses tumor immunity	3,52E-01	4,63E-01	7,95E-01	9,76E-01	3,62E-01	4,78E-01	Paired t-test
IL7	OID00761	P13232	Promotes tumor immunity	1,61E-01	3,03E-01	7,92E-01	9,76E-01	9,26E-02	2,24E-01	Paired t-test
IL8	OID00752	P10145	Chemotaxis; Suppresses tumor immunity; Vascular and tissue remodeling	4,31E-01	5,22E-01	7,94E-01	9,76E-01	4,59E-01	5,35E-01	Paired t-test
KIR3DL1	OID05550	P43629	Suppresses tumor immunity	3,10E-01	4,23E-01	9,78E-01	9,94E-01	1,67E-01	3,02E-01	Paired t-test
KLRD1	OID00839	Q13241	Promotes tumor immunity	3,18E-02	9,91E-02	3,75E-01	7,53E-01	4,64E-02	1,75E-01	Paired t-test
LAG3	OID05553	P18627	Suppresses tumor immunity	2,09E-01	3,44E-01	4,35E-01	8,18E-01	3,30E-01	4,68E-01	Paired t-test
LAMP3	OID00826	Q9UQV4	Suppresses tumor immunity	1,37E-02	7,40E-02	1,71E-01	6,18E-01	4,19E-02	1,75E-01	Paired t-test
LAP TGF-beta-1	OID00785	P01137	Suppresses tumor immunity	5,07E-01	5,81E-01	9,38E-01	9,94E-01	4,47E-01	5,34E-01	Paired t-test
MCP-1	OID00765	P13500	Chemotaxis; Vascular and tissue remodeling	2,34E-01	3,63E-01	7,53E-01	9,76E-01	2,13E-01	3,44E-01	Paired t-test
MCP-2	OID00795	P80075	Chemotaxis	1,67E-01	3,03E-01	6,66E-01	9,76E-01	1,80E-01	3,11E-01	Paired t-test
MCP-3	OID00755	P80098	Chemotaxis	5,74E-02	1,47E-01	7,33E-02	4,85E-01	2,10E-01	3,44E-01	Paired t-test
MCP-4	OID00768	Q99616	Chemotaxis; Suppresses tumor immunity; Vascular and tissue remodeling	3,13E-01	4,23E-01	3,52E-01	7,53E-01	5,06E-02	1,75E-01	Paired t-test
MIC-A/B	OID00820	Q29983,Q29980	Suppresses tumor immunity	5,31E-01	5,89E-01	9,46E-01	9,94E-01	4,13E-01	5,14E-01	Paired t-test
MMP12	OID00829	P39900	Suppresses tumor immunity; Vascular and tissue remodeling	1,93E-01	3,26E-01	5,53E-01	9,42E-01	2,35E-01	3,73E-01	Paired t-test
MMP7	OID00814	P09237	Apoptosis/cell killing; Suppresses tumor immunity	8,72E-02	1,96E-01	3,06E-01	7,53E-01	1,74E-01	3,08E-01	Paired t-test
MUC-16	OID05549	Q8WXI7	Suppresses tumor immunity	8,67E-04	1,14E-02	3,95E-03	9,08E-02	8,07E-02	2,12E-01	Paired t-test
NCR1	OID00816	O76036	Promotes tumor immunity	5,14E-01	5,81E-01	9,89E-01	9,94E-01	3,76E-01	4,87E-01	Paired t-test
NOS3	OID00777	P29474	Vascular and tissue remodeling	9,61E-01	9,71E-01	1,93E-01	6,34E-01	2,51E-01	3,85E-01	Paired t-test
PD-L1	OID00799	Q9NZQ7	Suppresses tumor immunity	9,36E-03	6,69E-02	2,25E-01	6,56E-01	1,60E-02	1,00E-01	Paired t-test
PD-L2	OID00831	Q9BQ51	Suppresses tumor immunity	1,20E-01	2,45E-01	7,63E-01	9,76E-01	2,77E-02	1,42E-01	Paired t-test
PDCD1	OID00791	Q15116	Suppresses tumor immunity	1,80E-03	1,81E-02	9,65E-02	5,22E-01	8,26E-03	7,44E-02	Paired t-test
PDGF subunit B	OID00790	P01127	Vascular and tissue remodeling	1,93E-01	3,26E-01	4,79E-01	8,64E-01	2,50E-01	3,85E-01	Paired t-test
PGF	OID00762	P49763	Vascular and tissue remodeling	1,95E-01	3,26E-01	9,93E-01	9,94E-01	1,10E-01	2,38E-01	Paired t-test
PTN	OID00823	P21246	Vascular and tissue remodeling	3,84E-01	4,72E-01	2,92E-01	7,53E-01	7,00E-01	7,49E-01	Paired t-test
TIE2	OID00754	Q02763	Vascular and tissue remodeling	2,14E-01	3,45E-01	6,09E-01	9,76E-01	6,11E-02	1,75E-01	Paired t-test
TNF	OID05554	P01375	Promotes tumor immunity; Suppresses tumor immunity; Vascular and tissue remodeling	2,57E-01	3,81E-01	7,49E-01	9,76E-01	2,72E-01	4,04E-01	Paired t-test
TNFRSF12A	OID00810	Q9NP84	Apoptosis/cell killing; Vascular and tissue remodeling	1,97E-02	9,52E-02	1,45E-01	5,87E-01	7,36E-02	1,99E-01	Paired t-test
TNFRSF21	OID00818	O75509	Apoptosis/cell killing	4,88E-02	1,28E-01	2,45E-02	3,22E-01	4,84E-01	5,43E-01	Paired t-test
TNFRSF4	OID00819	P43489	Promotes tumor immunity	3,23E-02	9,91E-02	3,44E-01	7,53E-01	4,02E-02	1,75E-01	Paired t-test
TNFRSF9	OID00753	Q07011	Promotes tumor immunity	2,93E-02	9,91E-02	1,44E-01	5,87E-01	1,14E-01	2,38E-01	Paired t-test
TNFSF14	OID00787	O43557	Promotes tumor immunity	3,71E-01	4,71E-01	9,05E-01	9,94E-01	3,05E-01	4,38E-01	Paired t-test
TRAIL	OID00769	P50591	Apoptosis/cell killing	1,40E-03	1,62E-02	7,38E-02	4,85E-01	8,90E-03	7,44E-02	Paired t-test
TWEAK	OID00789	O43508	Apoptosis/cell killing; Vascular and tissue remodeling	3,10E-01	4,23E-01	1,49E-01	5,87E-01	6,95E-01	7,49E-01	Paired t-test
VEGFA	OID00832	P15692	Vascular and tissue remodeling	9,01E-02	1,97E-01	4,43E-02	3,70E-01	4,53E-01	5,34E-01	Paired t-test
VEGFR-2	OID00780	P35968	Vascular and tissue remodeling	6,88E-02	1,67E-01	5,68E-01	9,50E-01	5,99E-02	1,75E-01	Paired t-test

Supplementary Table S2: Gene lists used for the RNA-based estimation of immune cell populations. Gene lists were obtained from[14], except gene markers for CD4 T-cells, which were obtained from[13].

Immune cell population	Gene list
B cells	*MS4A1, SPIB*
CD4+ T cells	*AMIGO2, CD40LG, ICOS, IGFBP4, ITM2A, TRAT1*
CD45	*PTPRC*
CD8+ T cells	*CD8A, CD8B*
Cytotoxic cells	*CTSW, GNLY, GZMA, GZMB, GZMH, KLRB1, KLRD1, KLRK1, NKG7, PRF1*
Dendritic cells	*CCL13, CD209, HSD11B1*
Exhausted CD8+ T cells	*CD244, EOMES, LAG3, PTGER4*
Macrophages	*CD163, CD68, CD84, MS4A4A*
Mast cells	*CPA3, HDC, MS4A2, TPSAB1, TPSB2*
Neutrophils	*CSF3R, FCGR3B, FPR1, SIGLEC5*
NK CD56- cells	*IL21R*
NK cells	*XCL1*
T cells	*CD3D, CD3E, CD3G, CD6, SH2D1A, TRAT1*
T_H1 cells	*TBX21*
Tregs	*FOXP3*

Supplementary Materials and Methods

Clinical samples

Tumor biopsies were either dry-frozen or fresh frozen (FF) embedded in TissueTek OCTTM Compound (Sakura Finetek), snap-frozen in liquid nitrogen and stored at -80ºC or obtained from formalin fixed paraffin embedded (FFPE) samples. Blood samples from all patients were stored in EDTA tubes at -80ºC. Urine supernatants were centrifuged and stored at -80ºC. Urine samples for protein analyses were sampled at a maximum of four months before and after BCG treatment.

DNA and RNA extraction

Tumor DNA from FF and dry-frozen tumors was extracted with Gentra Puregene Tissue Kit (Qiagen). DNA from FFPE samples was extracted using AllPrep DNA/RNA Kit (Qiagen). From peripheral blood, leukocyte DNA for germline (GL) reference was extracted using Qiasymphony DSP DNA midi kit (Qiagen) for all patients. Total Tumor RNA was extracted using RNeasy Mini and Micro Kits (Qiagen).

From tumors, haematoxylin and eosin (HE) stained sections of 4 µm were included to estimate carcinoma cell percentage.

DNA and RNA from tumors were extracted from serial cryosections of 20-25 µm. DNA from FFPE tumor specimens was extracted using punches taken from areas of the tumor with high estimated carcinoma cell percentage.

Urine (20–50 ml) was centrifuged at 3000G for 10 minutes, and supernatants were stored at –80C. Urine samples were thawed on ice, 10µl of urine was stored for Olink proteomics analyses (described below), PBS was added to remaining urine for a total volume of 4ml, and samples were centrifuged at 3000G for 10 minutes. Total cell-free DNA (cfDNA) was extracted from a median of 3.6 ml urine supernatants (range 0.7–3.65 ml). 10% ATL lysis buffer (median: 400µl, range: 100µl-500µl) (Qiagen, Aarhus, Denmark) was added, samples were incubated for 1.5-2h at room temperature followed by centrifugation at 1300G for 10 minutes. cfDNA extraction was performed using the QIAsymphony DSP Circulating DNA Kit (Qiagen). DNA was eluted in 60 µl ddH2O in DNA lobind tubes (Sigma-Aldrich).

Design of custom panel for targeted sequencing

For deep targeted sequencing of tumor specific mutations, we designed NGS panels where unique mutations (n=10-71) from 154 patients were included. Single nucleotide variants (SNVs) for the panels were selected from tumor guided WES analysis. Three panels covering mutations from 48, 54, and 52 patients, respectively, were designed.

SNVs were included based on the following criteria: 1. High or moderate impact mutations were favored. 2) Mutations with high variant allele frequencies (VAFs). 3) Mutations in known oncogenic genes from OnkoKB. 4) Bladder cancer associated genes (The Cancer Genome Atlas[1,2], MSKCC cBioPortal for Cancer Genomics[3,4], Uromol 2021[3,4], and Lamy *et al*[5]). 5) Mutations in the most exonically variable genes, reported by the Ingenuity Variant Analysis (IVA) software and/or at error-prone positions/in commonly reported erroneous contexts (C>T) were excluded, unless present in cancer driver genes or known bladder cancer genes. The three panels differed slightly in mutation selection.

Library preparation, deep-targeted sequencing and Mutation Calling of urinary

NGS libraries of cfDNA from urine supernatant were prepared using a modified version of the Mechanical Fragmentation Library preparation kit from Twist Bioscience in order to increase small fragment preservation and increase conversion rate. For robust error correction, 9 bp Unique Molecular Identifiers (UMI) were incorporated by replacing the twist adaptors with xGen™ UDI-UMI Adapters (Integrated DNA Technologies). The maximum cfDNA input was set to 100ng with no lower limit. Target enrichment was conducted using a modified version of the Twist Target Enrichment Protocol (Twist Bioscience) in combination with custom Twist panels (each SNV was captured by 120 bp probes on both strands). UMI consensus base calls were called using the fgbio tool package (v1.4.0). The ClipBAM (Hard-clipping) function of fgbio was enabled to avoid double count of variant calls of reads from the same template by clipping overlap between the reads. This was used for calculating UMI family size and UMI read depth. For UMI consensus collapsing, three reads were required as minimum and an editing distance of one was allowed. However, for secondary alignments, reads were not clipped. Realignment at INDEL positions were made using abra2 (v2.24). DeepSNV[6] was applied for detection and quantification of low-frequency tdDNA mutations in urine samples.

Calculations of UMI consensus read depth and UMI family sizes were based on the fgbio tool package (v1.4.0) that was run with the ClipBAM (Hard-clipping) function. Realignment at

INDEL positions are made using abra2 (v2.24). For UMI consensus collapsing, three reads were required as minimum and an editing distance of one was allowed.

Reads were mapped against the hg38 genome using bwa mem v.0.7.17. Mapped reads were grouped and consensus reads were generated from UMIs. Hereafter, read counts for the positions included in the panel were evaluated using the pileup tool bam read count. Only mutations detected in both the 5'-3' direction and the 3'-5' direction were included. Furthermore, at least three reads with different UMIs supporting a given mutation were required.

Copies per ml were calculated as follows:
GE/ml = (DNA input(ng)*VAF*(1000 pg/ng)/(3.3pg/GE))/urine (ml)
Clearance of tumor derived DNA (tdDNA) was defined as VAF ≠ 0 in pre-BCG samples and VAF=0 in post-BCG samples.

Neoantigen Calling

HLA types were called using POLYSOLVER[7], xHLA[8], and OptiType[9], with patient HLA type decided by consensus vote supported by at least two algorithms. If no majority could be reached, POLYSOLVER was used. All novel 9-11mer peptide fragments were generated by MuPeXI[10] and eluted ligands (EL) rank-percentage scores for all HLA alleles were predicted by NetMHCpan-4.1[11]. The rank-percentage score represents the rank of the fragments EL probability compared to a set of random natural peptides. A mutation was considered a neoantigen if at least one fragment had an EL rank percentage score<2%, for at least one HLA allele.

DeepSNV

The inclusion of genomic positions associated with multiple patients on every custom panel, facilitates an abundance of sequencing data for every genomic position with no mutations expected to be present. We exploited this by employing an analysis framework based on a maximum likelihood implementation of the shearwater algorithm developed by Gerstung *et al*.[6]. In brief, a background error model was built by fitting presumably non-mutated data, i.e. data from all samples not associated with a given mutation, to a binomial distribution with site-specific calculation of the dispersion for every mutation of interest. Samples with a VAF at a given position above 25% were excluded when generating the error model. Similarly, samples with a read depth below 50 at a given position were excluded when generating the error model. Furthermore, positions with an average error-rate above 10% across presumably non-mutated samples were excluded. Presumably mutated data, i.e. data from

the target positions of a given sample, was assessed for a statistical significant difference compared to the background error model. Resulting *p*-values were corrected for multiple testing using the Benjamini-Hochberg procedure and adjusted *p*-values below 0.05 were considered significant.

In addition, to exploit that data were generated for all positions in a custom panel for every sample, we established an analysis to assess the combined signal from all target positions for a given sample. We used Fisher's method to calculate the sum of logs for all *p*-values obtained when analyzing the target positions. To gauge a randomly expected level of signal, we randomly sampled the same number of mutations as the target positions from non-target positions and similarly calculated the sum of logs. This was performed 10,000 times. Only samples with a sum of log scores greater than all scores from random sampling were considered ctDNA positive.

RNA sequencing data

Salmon[12] was used to quantify the expression of transcripts using annotation from the Gencode release 33 on genome assembly GRCh38.

Spiderplots were generated using the Radarchart function in the R package fmsb.

We estimated immune cell populations from the RNA-seq data using established gene expression signatures as in Rosenthal *et al.*[13–15]. A score for each immune cell population was calculated as the mean expression of all marker genes for the given cell type and a total immune score was defined as the mean of all immune cell population scores. Individual scores for B-cells, neutrophils and NK-cells were not evaluated as genes were missing for these cell population signatures. Gene lists are available in Supplementary Table S3.

WES analyses

MutationalPatterns was used for *de novo* extraction of mutational signatures[16,17]

References

1. Robertson, A. G. *et al.* Comprehensive Molecular Characterization of Muscle-Invasive Bladder Cancer. *Cell* **174**, 1033 (2018).
2. Cancer Genome Atlas Research Network. Comprehensive molecular characterization of

urothelial bladder carcinoma. *Nature* **507**, 315–322 (2014).

3. cBioPortal for Cancer Genomics. https://www.cbioportal.org/.
4. Lindskrog, S. V. *et al.* An integrated multi-omics analysis identifies clinically relevant molecular subtypes of non-muscle-invasive bladder cancer. *Urology* (2020) doi:10.1101/2020.06.19.20054809.
5. Lamy, P. *et al.* Paired Exome Analysis Reveals Clonal Evolution and Potential Therapeutic Targets in Urothelial Carcinoma. *Cancer Res.* **76**, 5894–5906 (2016).
6. Gerstung, M. *et al.* Reliable detection of subclonal single-nucleotide variants in tumour cell populations. *Nat. Commun.* **3**, 811 (2012).
7. Shukla, S. A. *et al.* Comprehensive analysis of cancer-associated somatic mutations in class I HLA genes. *Nat. Biotechnol.* **33**, 1152–1158 (2015).
8. Xie, C. *et al.* Fast and accurate HLA typing from short-read next-generation sequence data with xHLA. *Proc. Natl. Acad. Sci. U. S. A.* **114**, 8059–8064 (2017).
9. Szolek, A. *et al.* OptiType: precision HLA typing from next-generation sequencing data. *Bioinformatics* **30**, 3310–3316 (2014).
10. Bjerregaard, A.-M., Nielsen, M., Hadrup, S. R., Szallasi, Z. & Eklund, A. C. MuPeXI: prediction of neo-epitopes from tumor sequencing data. *Cancer Immunol. Immunother.* **66**, 1123–1130 (2017).
11. Reynisson, B., Alvarez, B., Paul, S., Peters, B. & Nielsen, M. NetMHCpan-4.1 and NetMHCIIpan-4.0: improved predictions of MHC antigen presentation by concurrent motif deconvolution and integration of MS MHC eluted ligand data. *Nucleic Acids Res.* **48**, W449–W454 (2020).
12. Patro, R., Duggal, G., Love, M. I., Irizarry, R. A. & Kingsford, C. Salmon provides fast and bias-aware quantification of transcript expression. *Nat. Methods* **14**, 417–419 (2017).
13. Davoli, T., Uno, H., Wooten, E. C. & Elledge, S. J. Tumor aneuploidy correlates with markers of immune evasion and with reduced response to immunotherapy. *Science* **355**, (2017).

14. Danaher, P. *et al.* Gene expression markers of Tumor Infiltrating Leukocytes. *J Immunother Cancer* **5**, 18 (2017).
15. Rosenthal, R. *et al.* Neoantigen-directed immune escape in lung cancer evolution. *Nature* **567**, 479–485 (2019).
16. Manders, F. *et al.* MutationalPatterns: the one stop shop for the analysis of mutational processes. *BMC Genomics* **23**, 134 (2022).
17. Blokzijl, F., Janssen, R., van Boxtel, R. & Cuppen, E. MutationalPatterns: comprehensive genome-wide analysis of mutational processes. *Genome Med.* **10**, 33 (2018).